

# A Preliminary Study on Laser Surface Texturing of Passenger Car Engine Piston Rings

**Gábor Laki**

Assistant Lecturer  
Széchenyi István University  
Department of Propulsion Technology  
Hungary

**Gergely Kovács**

Technical Assistant  
Széchenyi István University  
Hungary

**Attila Schweighardt**

Assistant Lecturer  
Széchenyi István University  
Department of Whole Vehicle Development  
Hungary

**András Lajos Nagy**

Research Fellow  
Széchenyi István University  
Department of Propulsion Technology  
Hungary

*Laser surface texturing offers a possible solution for reducing friction between sliding surfaces in engineering applications. Optimized surface topography can also contribute to reduced wear and elevated longevity by modifying the load and speed-dependent friction state in a system. This preliminary experimental study investigates the applicability of affordable fibre laser marking systems for microtexturing piston rings, in order to achieve a measurable reduction in friction under subsystem model conditions. A selection of textures are applied to chromium-coated cast iron piston rings. The resulting surface topographies are characterized through confocal microscopy and subjected to friction testing. A correlation analysis is conducted on surface topography parameters to identify key laser process parameters. Findings indicate an improvement in the range of 7-8% in terms of friction coefficient with appropriate texture size.*

**Keywords:** microtexture, Laser ablation, surface texturing, friction reduction, piston ring.

## 1. INTRODUCTION

Laser technology has revolutionized various fields of engineering and is extensively used in industries such as automotive, aerospace, manufacturing, and biomedical engineering, offering numerous advantages over traditional techniques. Particularly in mechanical engineering fields, laser applications have been highly impactful, allowing the controlled modification of surface topology and material properties. Lasers enable engineers to modify surface topologies by selectively removing (ablation) or adding (cladding and direct metal sintering) material and generating precise micro- or nanostructures (texturing). With the precise energy delivery of laser techniques, surfaces can be tailor-made to increase adhesion, modify wetting behaviour, and optimize friction in sliding contacts.

Taking a look at the scientific literature, a wide variety of successful engineering application examples can be found for laser-based manufacturing techniques. Laser ablation has been successfully used to create special materials [1], alter surface hardness [2] and increase wear resistance of components [3]. Several influencing factors affect the outcome of laser surface treatment technologies, e.g., base material, laser wavelength, duration, energy, focusing or angle of incidence. Chen et al. [4] experimented with laser fluence on a femtosecond laser to seek the best ablation performance. Optimal laser fluence was found to be highly dependent on base material properties. Jia et al. [5] experimented with sub-microsecond lasers to establish a fast and high-quality drilling process on ceramics. Findings show a

direct correlation between bore quality and speed, due to shortened heat affection and thus reduced material damage with increased lasing speed. Yan et al. [6] experimented with continuous high-energy lasers to understand the ablation process of ferrous metals. As reported, laser irradiation melts steel in an initial puddle that grows over time until the sample is fully penetrated. The molten steel vaporizes during the process at about 3x higher temperature than the melting point of solid steel. The ablation is also accompanied by molten material splashing. Cheng et al. [7] observed the emergence of residual compressive and tensile stresses due to extensive heat introduction to the material during laser cladding. The phenomenon was traced to dissimilar grain structures as a result of the temperature gradient in the melt pool.

For texturing applications, laser process parameters have a significant effect on the produced surface properties. Lu et al. [8] experienced elevated surface roughness and groove width with decreasing groove depth as the incident angle decreased. Implementing laser ablation to create different types of surface textures can enhance friction properties [9] and alter adhesion between the base surface and a coating. Caraguay et al. [10] created grooved and grid patterns on steel samples and successfully improved the adhesion of an anti-corrosion epoxy coating. Particularly for automotive applications, suitable laser surface texturing of running surfaces can offer lower fuel consumption and reduced emissions [11]. The technology is not limited to traditional industrial applications, as it has been successfully applied to bio-implants to increase cellular growth and adhesion [12].

With the increasing availability and decreasing cost of laser ablation equipment, previously unfeasible concepts can be investigated in numerous industries. Laser surface texturing has been successfully applied to cylinder bores in the past, to achieve oil retention and

Received: February 2025, Accepted: March 2025

Correspondence to: Gabor Laki, Assistant lecturer  
Department of Propulsion Technology, Széchenyi  
István University, H-9026 Győr, Egyetem tér 1, Hungary  
E-mail: laki.gabor@sze.hu

doi: 10.5937/fme2502252L

© Faculty of Mechanical Engineering, Belgrade. All rights reserved

FME Transactions (2025) 53, 252-259 252

improve friction [13]. Regarding serviceability and longevity, texturing piston rings as opposed to the cylinder could contribute to reasonable improvements, with moderate added cost. [14-16].

Introducing engineered topological features on the micrometre scale affects friction in a tribosystem through a complex set of mechanisms. [17] Microscopic features, e.g., dimples can both trap wear debris and act as lubricant reservoirs, contributing to a reduction of friction through reducing the occurrence of three-body abrasion and acting as local lubricant sources under starved lubrication. Furthermore, micro texturing reduces the effective area of contact, which decreases the number of asperity contacts in the mixed lubrication regime. Microtextures also alter the pressure distribution in the lubricant between contacting surfaces, creating a pressure gradient that contributes to an elevated load-bearing capacity of the fluid film. Cavitation plays a significant role in achieving a favourable pressure gradient. [18,19] However, micro texturing can have a negative impact as well, since it disrupts the laminar near-wall flow of the lubricant and therefore contributes to elevated fluid friction under higher relative velocities. [20] Together, these phenomena have a measurable impact on friction, which can be visualized on the Stribeck curve, as presented in Figure 1.

Friction and wear experiments using controlled model environments present a solution for high throughput testing of various phenomena in tribology, e.g., friction reduction through surface microstructure. Tribometer testing also plays a critical role in evaluating the friction and wear behaviour of various material combinations. [21] An alternating tribometer resembles the kinematics of internal combustion engine pistons, enabling a simplified assessment of the piston ring and cylinder tribosystem. [22] This method is also effective in analyzing the impact of lubricants on system performance. [23] Paulovics et al. [24] recommend fabricating tribometer specimens from actual engine components to ensure representative material interactions, surface hardness, and topography.

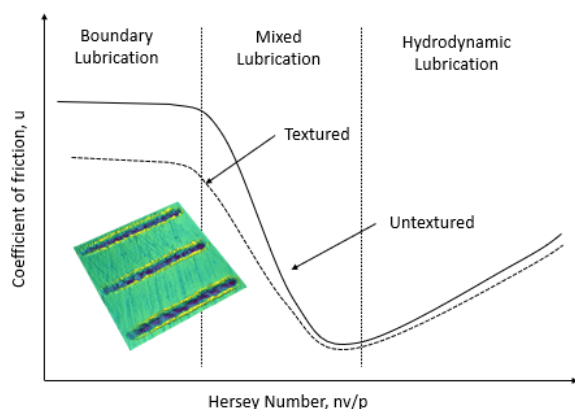


**Figure 1. The effect of surface texturing on the Stribeck curve, based on [20]**

### 1.1 Novelty of the current study

Although several papers have touched on the topic of laser surface texturing functional components, as well as surface texturing either or both the cylinder liner and the

piston ring, there are some shortcomings in the available literature, specifically regarding the analysis of laser-manufactured surface texture topographies, and the investigation of friction force along the stroke in a reciprocating system. Ezhilmaran et al [25] conducted experiments using a pulsed nanosecond Nd<sup>3+</sup>:YAG to manufacture dimples on moly-chrome ceramic film coated piston rings. Although a thorough analysis was conducted including the investigation of texture parameters using both tribometric measurements and numerical analysis, the approach is based on Nd<sup>3+</sup>:YAG technology, which generally offers lower efficiency, lower beam quality and higher associated costs with regular lamp replacement compared to fibre lasers. Urabe et al [26] investigated surface texturing on the cylinder liner using a motored floating liner friction testing rig and engine bench tests. The study highlights favourable effects on friction losses, oil film thickness and fuel consumption, but utilizes texturing in the middle of the stroke, neglecting the potential benefits of surface texturing under the most severe conditions around the top dead centre. Rao et al [27] introduce laser surface texturing on both the cylinder liner and the piston ring of an internal combustion engine in various configurations and compare wear mass loss, exhaust gas temperature and NO<sub>x</sub> emissions under fired engine conditions. However, the study presents no data on friction performance, nor on the topography characteristics of the laser-manufactured surface textures, which would help the understanding of how better performance metrics are achieved with the textured engine parts. Patil et al [28] conducted friction and wear experiments on a reciprocating tribometer to assess laser texturing on the piston ring of a 0.8 L internal combustion engine. The study reports extensively on the average coefficient of friction and wear mass loss, but lacks insight regarding friction along the stroke, as well as a detailed analysis of manufactured laser surface texture topography. Yin et al [29] performed both numerical and experimental studies on the application of laser-manufactured micro dimple arrays on the cylinder liner of an internal combustion engine. The study highlights the effect of surface texturing on the pressure field in the lubricant between the contact pair, and reports motored torque with various texture configurations. On the other hand, no detailed study is concluded regarding the manufactured shapes, and motored torque is only reported at discrete engine speeds, and not as a function of the stroke.

The present study aims to explore the potential of reducing friction in the piston ring–cylinder liner system by micro texturing the ring through laser ablation on a selection of affordable 355 nm and 1064 nm wavelength fibre laser marker machines, unlike most existing research, which predominantly focuses on high-performance femtosecond lasers or cheap, but less precise Nd:YAG equipment for surface texturing. Furthermore, this study emphasizes the effect of texturing as a function of movement along the stroke of a reciprocating machine, and presents an in-depth look on the manufactured surface topography, to better understand the underlying phenomena and practical effects resulting from the utilized manufacturing technology.

## 2. METHODOLOGY

The experimental design of this study relies heavily on available materials and equipment. The core hypothesis of the project laments the possibility of achieving consistent and repeatable friction reduction in a model piston ring–cylinder liner environment (i.e.: tribometer experiment), through micro texturing the piston ring surface on an affordable fibre laser marker.

To assess the above, a variety of textures were created on chromium-coated piston ring segments using IR fibre and UV lasers. Texture shape and size were selected based on previous experience and literature review. Manufactured texture shapes were investigated using confocal microscopy. Surfaces with close to ideal texture shapes were tested on a reciprocating tribometer to ascertain the friction coefficient during lubricated sliding. Well-performing textures were replicated multiple times on a selected laser machine to evaluate reproducibility.

### 2.1 Laser equipment, materials, texture shape

A groove texture shape with a nominal width and length of  $40 \times 500 \mu\text{m}$ , a nominal vertical spacing of  $200 \mu\text{m}$ , and a nominal horizontal spacing of  $100 \mu\text{m}$  was selected based on prior literature analysis performed by Laki et al. [30], Azmi et al. [31] and Pawlus et al [13]. The depth of the texture was varied in the range of  $0.5 - 6 \mu\text{m}$ , while laser parameters (e.g., laser power, repetition rate, feed rate) were also varied, to assess their effect on the resulting texture. A total of more than 50 individual textures were manufactured during the study. Figure 2. showcases an as-manufactured untextured ring (top), a ring after being microtextured (middle), and the worn configuration of a microtextured ring (bottom).

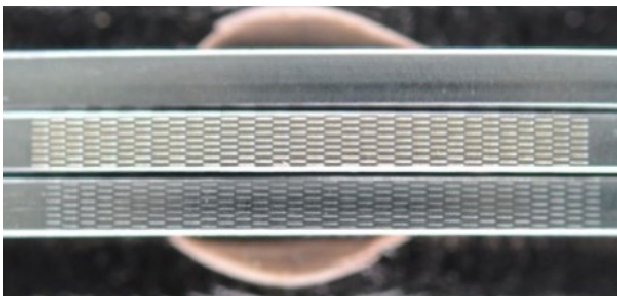


**Figure 2.** The running surface of the piston ring segments shows the untextured (upper) and textured (middle) configuration, as well as the textured surface after tribometer testing (lower)

**Table 1.** Laser equipment utilized for the micro texturing experiments

ID	Type	Wavelength	Power
UV1	SX 5005	355 nm	5 W
UV2	SX 5003	355 nm	3 W
IR1	SX 5050	1064 nm	50W
IR2	SX 5030	1064 nm	30 W

DIN EN 60825-1 [32] compliant UV and fibre lasers have been applied to ablate the surface of chromium-coated cast iron piston ring segments to create the desired texture geometry. Table 1. summarizes the key

parameters of the utilized laser equipment. IR2 was used to reproduce good-performing textures in the later stages of the study. Laser equipment was kindly provided by EERS-Hungary Kft. for the study.

Goetze GDC 50 chromium-coated piston rings used in passenger car engines were selected as the foundation of the study. As-manufactured ring surfaces were measured to establish initial surface roughness. A mean arithmetic surface roughness ( $R_a$ ) of  $0.0895 \mu\text{m}$  and a ten-point height of irregularities ( $R_z$ ) of  $0.55 \mu\text{m}$  was determined. Piston rings were cut into 33 mm long sections on a laboratory sectioning machine. Texturing was applied in the centre region of each ring. The length of the textured area was 16 mm. The counter-body for friction experiments were cylinder segment specimens made from GJV-450 vermicular graphite cast iron. Cylinder segments were manufactured from the crankcase of a turbocharged direct injection engine using electrical discharge machining and finished on a CNC mill. A mean arithmetic surface roughness ( $R_a$ ) of  $0.489 \mu\text{m}$  and a ten-point height of irregularities ( $R_z$ ) of  $3.87 \mu\text{m}$  was established. Due to the necessary segment length for fastening in the tribometer, each cylinder specimen has room for two independent test runs on its surface.

### 2.2 Surface metrology and friction assessment

The developed surface textures were evaluated on a DCM3D confocal measuring microscope produced by Leica Microsystems GmbH (Wetzlar, Germany). A 20X HCX PL FLUOTAR lens was used with a 0.50 numeric aperture to capture extended topography slides in a measurement area of  $1.66 \times 1.24 \text{ mm}$ . The selected lens allows fast assessment of large surface areas without sacrificing detail on the investigated topographic features. Collected topography slides were processed using LeicaMAP 6.2 (Digital Surf, Besançon, France) to level the surfaces, fill in non-measured points, and remove surface waviness before calculating standard surface roughness parameters according to ISO 25178 [33]. Furthermore, LeicaMAP was also used to generate single cross-sections, cross-section envelopes, and height-coded 3D topography renders of the surfaces.

Textured samples were subjected to friction analysis on a TE-77 High-Frequency Friction Machine (Phoenix Tribology Ltd., Berkshire, England, see Figure A1. in the appendix). The test setup is introduced on Figure 3.

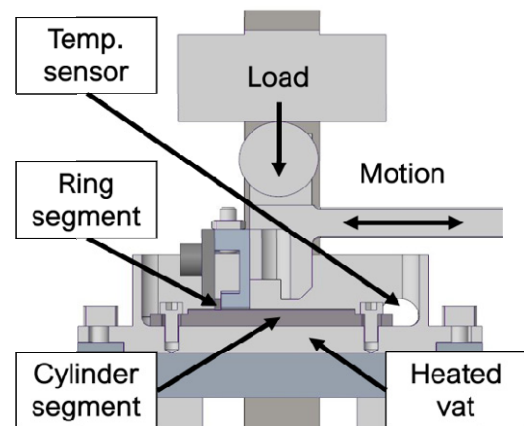


**Figure 3.** Schematics of the ring-liner model system in the TE-77 High-Frequency Friction Machine [34]

Laser-textured piston ring segments were fastened in the upper (oscillating) sample holder, which was also used to apply a predefined load to the friction pair. Cylinder segments acting as counter-bodies were mounted into the stationary lower sample holder (heated vat), which is also responsible for the temperature conditioning of both specimens and the utilized lubricant. Each friction test is run for 120 minutes at 20 Hz motion frequency, with a 10.4 mm stroke and 200 N load. Lubrication is ensured through 8 ml of Shell PC1654 0W-30 engine oil, with the vat heated to 100°C.

The following values were measured during the operation: friction force, alternating motion frequency, load, specimen temperature, and contact potential. The coefficient of friction is determined according to the Coulomb friction equation, as a ratio of the measured friction force and imposed normal force (load). Contact potential is a means of monitoring the friction state in the system. A 50-mV voltage is applied between the cylinder and ring segment, and potential difference is measured during friction and wear experiments. This potential difference rarely drops under 50 mV under expected working conditions. An onset of moderate wear or lack of lubricant quickly leads to an increase in asperity interactions, that result in a momentary flow of electricity, which is indicated by a decreased potential difference (i.e.: contact potential) value.

Roughness and topology evaluations were carried out in the Surface Analysis Laboratory, while friction measurements were done at the Tribology Laboratory at Széchenyi István University.

### 3. RESULTS AND DISCUSSION

The results of experimental surface texturing attempts were analysed regarding texture shape and friction reduction to evaluate the feasibility of producing functional surface textures with low-cost fibre laser equipment. An initial assessment of manufactured surface textures through confocal microscopy revealed obvious outliers, where the established microtexture was barely distinguishable from the original surface texture or the created grooves had excessive spatter along the edges. These outliers were discarded from further assessment. As a result, a total of 44 individual microtexture configurations were tested on the tribometer.

A box plot of measured friction coefficients with the tested microtextured piston rings is presented in Figure 4. as a concise summary of preliminary testing. Textures are categorized into 3 bins, based on the achieved friction reduction. Samples achieving a reduction in the coefficient of friction above 3% were labelled “better”, samples between -3% and 3% reduction were labelled “neutral”, and samples below -3% reduction were labelled “worse”.

#### 3.1 Texture shape and performance assessment

The highest achieved reduction in coefficient of friction was 7.79%, meanwhile, the largest friction increase was 7.06%. A high number of investigated texture configurations yield neutral, or disadvantageous friction states. Figure 5. presents average profiles and envelopes of the

surfaces corresponding to the best and worst achieved coefficient of friction, along with a neutral performing surface. Figure 5. also highlights the cause of the negative effect, which can be traced back to spattering, i.e., the appearance of relatively tall asperities on the boundaries of the manufactured grooves.

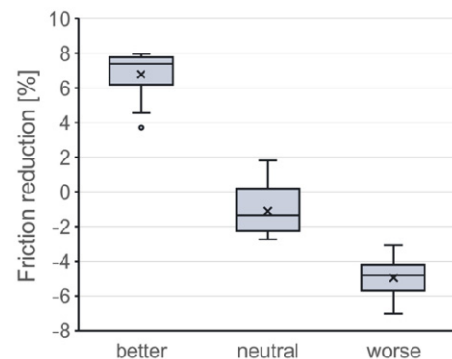


**Figure 4. Box plot of measured friction coefficients with the investigated microtextures, binned to “better” (> 3% improvement), “neutral” (between -3% and 3% improvement) and “worse” (< -3% improvement) categories.**

This is a common phenomenon in laser ablation applications and is explained by the observation of Yan et al. [10]. As the available laser power is insufficient for sublimation, a molten metal puddle is created, which has a significantly higher vaporization temperature. The metal pool then displaces according to the thermocapillary effect [35],[36], due to the temperature difference between the melt zone and the rest of the surface. The displaced material solidifies, and the resulting hills on the surface topography contribute to an increased roughness and ultimately to an increase in the coefficient of friction [37]. Neutral surfaces showcase indistinguishable texture traces; hence these have minimal effect on coefficient of friction.

Interestingly, the best-performing surface texture also displays moderate spatter. Compared to the worst, the apparent differences are the overall feature height and the width of grooves. Best-performing textures have a characteristic depth of ca. -4 μm, and a maximum asperity height of ca. 5 μm due to spatter. The characteristic groove width is nearly equal to the nominal beam diameter of 50 μm. In contrast, worst-performing textures have a characteristic depth well below -10 μm, and a maximum asperity height around 10 μm, while the groove width is typically below the nominal beam diameter.

#### 3.2 Texture reproducibility, friction response

To assess reproducibility, the best-performer texture configuration was replicated using the fibre laser IR2. The results of texturing experiments on samples 105L, 160L and 174UL depicted in Figure 6. show some asperities larger than 5 μm due to spatter. Characteristic groove widths of 50 μm were measured, which is close to the nominal beam diameter.

The grooves are well-defined, with a continuous valley between the groove boundaries. An average improvement of 7.1 % with a 1.3 % deviation was registered in term of coefficient of friction for the textured samples as a result of the reproducibility study.

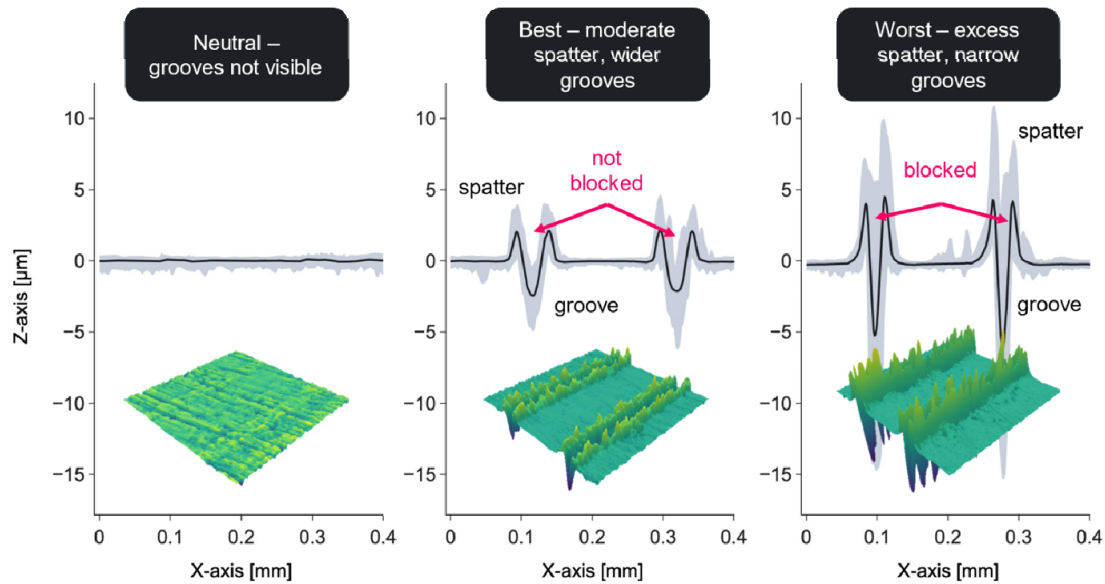


Figure 5. Average (solid black line) and envelope (grey filled area) of roughness profile series for neutral, best, and worst performing surface textures, with a corresponding surface snippet showcasing the topography

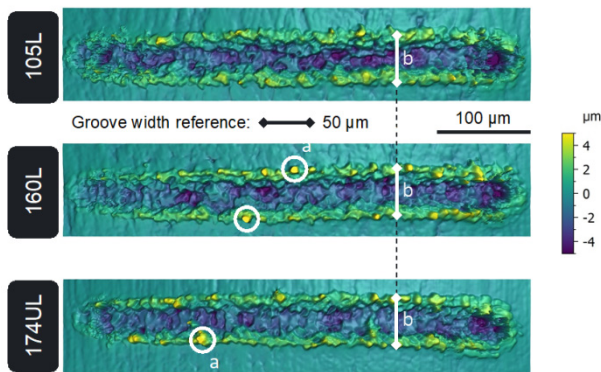


Figure 6. Typical groove topography from repeated texturing experiments showing samples 105L, 160L and 174UL. Some asperities larger than 5 μm can be found as a result of spatter (marked with “a”). Characteristic groove widths are close to the nominal beam diameter of 50 μm (marked with “b”).

To understand how the imposed texture affects the friction state, a detailed look was taken at the friction force progression using high-speed data acquisition during friction and wear testing. The utilized friction testing instruments are capable of registering friction force and current position at a 20 kHz acquisition rate, allowing for a depiction of friction force along the stroke resulting in the dynamic stroke friction response curve presented in Figure 7. High-speed acquisition data was saved for 5000 entries, which corresponds to 5 full strokes, considering 20 Hz motion frequency.

Comparing an untextured and textured ring’s friction response curve yields the following insight:

- Both curves follow a periodic pattern corresponding to the reciprocating motion of the sample, as anticipated,
- friction force rises steeply at stroke reversals ( $\sim \pm 4$  mm) for both the textured and untextured sample, however, the untextured ring displays somewhat higher peak friction force values,
- the textured sample shows slightly higher oscillations in the mid-stroke region.

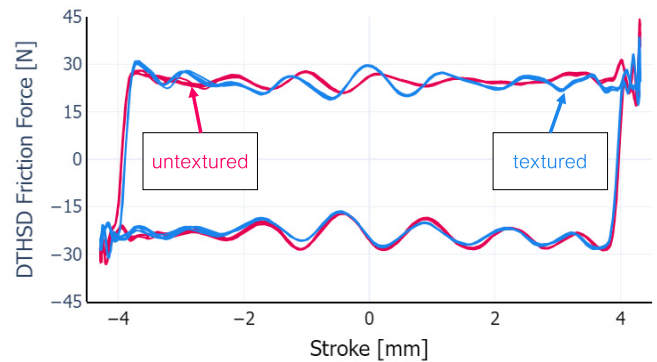


Figure 7. Dynamic stroke friction response curve of an untextured (red) and textured (blue) piston ring as a result of high-speed data acquisition during friction and wear testing, depicting the variation in friction force along the stroke.

Furthermore, the high-resolution acquisition of friction force and position also enables the calculation of friction work along a stroke by using the Simpsons formula. Since friction force values are stored as signed values due to the bi-directionality of the friction sensor, the absolute intermittent friction work values are taken and summed to obtain the total friction work for 5 strokes. The corresponding average friction work can then be given for both cases:

- untextured ring  $W_F = 711.7$  mJ / stroke
- textured ring  $W_F = 678.8$  mJ / stroke

Although the difference appears to be insignificant, it still amounts to a 4.62 % reduction in friction work, which is comparable to the reduction in coefficient of friction reported earlier. The disparity between friction work and friction coefficient can be attributed to the fact, that the reported coefficient is an extremum of values recorded during the 1-second accumulation window for low-speed acquisition, whereas the average friction work was calculated using a significantly larger number of values and is representative of the full stroke.

The TE77 High-Frequency friction machine can also monitor the friction state by applying a contact potential

– a 50 mV differential potential between the friction pair. When the two surfaces are isolated by an uninterrupted layer of lubricant, the measured value hovers around 50 mV – i.e., fully hydrodynamic lubrication. This value can drop below 49.5 mV when an asperity contact occurs either due to an abrupt change in velocity, that leads to the breakdown of the lubricant film, or a momentary bridging of the surfaces by metallic particles in the lubricant – i.e., wear debris.

A brief look at the high-speed contact potential data in Figure 8. further highlights the beneficial effect of surface micro texturing, especially around the reversal points. The measured value fluctuates between 49.5 mV and 50.5 mV, which indicates a mostly intact lubricant film. Reoccurring values below 49.5 mV are only characteristic of the untextured surface. The textured piston ring consistently stays over 49.5 mV at the reversal points, exhibiting a more favourable friction state.

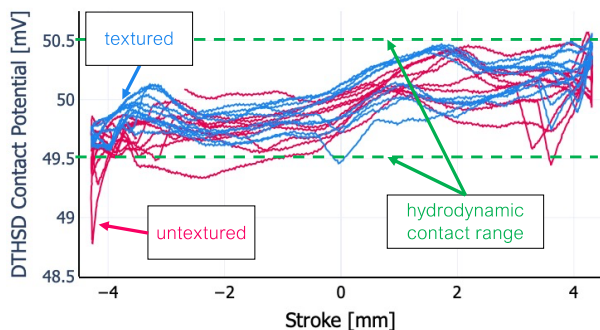


**Figure 8. Contact potential along the stroke for an untextured (red) and textured (blue) piston ring as a result of high-speed data acquisition during friction and wear testing, depicting the variation in the quality of lubrication.**

Both the friction response curve and the contact potential curve demonstrate a preferential behaviour of the microtextured surface over the as-manufactured reference surface topography.

#### 4. CONCLUSION

The study aimed to assess the feasibility of manufacturing microtextured surface modification on piston ring samples with affordable and accessible IR fibre laser tooling with the required reproducibility. The laser-textured specimens were subjected to friction and wear testing on a reciprocating rig and primarily evaluated based on their reduction in friction. Samples were also analysed using confocal microscopy to determine texture shape and correlate shape and friction loss. Based on the gathered experimental evidence, the following conclusion can be formulated:

- cheap nanosecond 1064 nm fibre laser marker/engraver machines are capable of producing functional surface textures within the range of  $\sim 5$   $\mu\text{m}$  depth, which facilitates the broader adoption of friction-reducing surface microtextures in complex engineering systems, e.g., select tribosystems of an internal combustion engine,
- even without systematic parameter optimisation, a friction reduction of 7.1% was achievable and reproducible on 3 samples with 1.3% deviation,

which could be further improved by utilizing e.g., a response surface method-based optimisation for fine-tuning texture parameters,

- best-performing surface textures typically showed a relatively shallow depth of 5  $\mu\text{m}$  compared to the 50  $\mu\text{m}$  width and 500  $\mu\text{m}$  length of the utilized texture shape, alongside moderate asperity growth at the boundaries of the shape,
- worst-performing textures generally showed a high asperity peak growth with  $>10$   $\mu\text{m}$  height as a result of excessive melting and relocation of the melt pool through thermocapillary effects, which are expected to be improved by introducing an inert atmosphere during laser texturing, and experimenting with defocusing the laser beam to better control ablation power,
- using surface micro texturing, the anticipated friction reduction was achieved by reducing the peak friction force at and around stroke reversals by maintaining a favourable friction state, as highlighted by the measured contact potential.

The presented study has its limitations, mainly due to equipment availability, which prevented the systematic analysis of laser parameters using robust evaluation methods, e.g., Design of Experiments. A structured approach would allow for an in-depth correlation analysis regarding the effect of not only laser power, repetition rate and feed rate but also defocusing and using an inert gas to assist the process. With precise control of these parameters, the unwanted phenomenon of asperity growth around texture edges (spatter) could be further reduced, which could lead to additional improvements in the coefficient of friction.

#### ACKNOWLEDGMENT

This article is published in the framework of the project "Production and Validation of Synthetic Fuels in Industry-University Collaboration", project number "ÉZFF/956/2022-ITM\_SZERZ".

The authors would like to thank the colleagues of the Tribology Laboratory of the Department of Propulsion Technology at Széchenyi István University, and the Surface Analysis Laboratory of the Department of Propulsion Technology at Széchenyi István University for their kind support in carrying out the tribometric measurements and surface analysis.

#### REFERENCES

- [1] Wang, S., Zhao, Z., Bai, P., Du, W., Li, L.: Effect of in situ synthesis TiC on the microstructure of graphene/Ti6Al4V composite fabricated by selective laser melting, *Mater Lett*, Vol. 304, No. August, p. 130715, 2021, doi: 10.1016/j.matlet.2021.130715.
- [2] Meng, Y., et al.: Thermochemical surface hardening of Ti-6Al-4V: On the role of temperature and treatment media, *Surf Coat Technol*, Vol. 422, No. May, p. 127505, 2021, doi: 10.1016/j.surfcoat.2021.127505.
- [3] Bushueva, E., Kuzin, P., Drobyaz, E., Grinberg, B.: Wear Resistance Increasing of Austenitic Steel by

- the Surface Hardening with Titanium Carbide, *Mater Today Proc*, Vol. 11, pp. 342–347, 2019, doi: 10.1016/j.matpr.2018.12.155.
- [4] Chen, H., et al.: Femtosecond laser ablation of dentin and enamel: relationship between laser fluence and ablation efficiency, *J Biomed Opt*, Vol. 20, No. 2, p. 028004, 2015, doi: 10.1117/1.jbo.20.2.028004.
- [5] Jia, X., Chen, Y., Liu, L., Wang, C., Duan, J.: *Advances in Laser Drilling of Structural Ceramics, Nanomaterials*, Vol. 12, No. 2, pp. 1–39, 2022, doi: 10.3390/nano12020230.
- [6] Yang, L., Wei, T., Lisheng, L., Junfeng, S., Ming, S., Xiangzheng, C.: Study on heat effect of high-power continuous wave laser on steel cylinder, *Applied Sciences (Switzerland)*, Vol. 10, No. 21, pp. 1–11, 2020, doi: 10.3390/app10217844.
- [7] Cheng, Y., et al.: Effects of laser energy density and path on residual stress of remanufactured key components for shield tunneling machine, *Mater Chem Phys*, Vol. 290, No. July, p. 126617, 2022, doi: 10.1016/j.matchemphys.2022.126617.
- [8] Lu, Y., Deng, J., Wu, J., Wang, R., and Meng, Y.: Influence of micro-grooves processed by laser with different incident angle on the properties of TiAlSiN coatings, *Surf Coat Technol*, Vol. 446, No. February, p. 128793, 2022, doi: 10.1016/j.surfcoat.2022.128793.
- [9] Vlădescu, S.C., Fowell, M., Mattsson, L., and Reddyhoff, T.: The effects of laser surface texture applied to internal combustion engine journal bearing shells – An experimental study, *Tribol Int*, Vol. 134, No. January, pp. 317–327, 2019, doi: 10.1016/j.triboint.2019.02.009.
- [10] Caraguay, S.J., Pereira, T.S., Giacomelli, R.O., Cunha, A., Pereira, M., and Xavier, F.A.: The effect of laser surface textures on the corrosion resistance of epoxy coated steel exposed to aggressive environments for offshore applications, *Surf Coat Technol*, Vol. 437, No. January, p. 128371, 2022, doi: 10.1016/j.surfcoat.2022.128371.
- [11] Tomanik, E., Profito, F., Sheets, B., and Souza, R.: Combined lubricant–surface system approach for potential passenger car CO<sub>2</sub> reduction on piston-ring-cylinder bore assembly, *Tribol Int*, Vol. 149, No. July 2018, p. 105514, 2020, doi: 10.1016/j.triboint.2018.12.014.
- [12] Xu, Y., et al.: Friction stability and cellular behaviors on laser textured Ti–6Al–4V alloy implants with bioinspired micro-overlapping structures, *J Mech Behav Biomed Mater*, Vol. 109, No. October 2019, p. 103823, 2020, doi: 10.1016/j.jmbbm.2020.103823.
- [13] Pawlus, P., Koszela, W., and Reizer, R.: Surface Texturing of Cylinder Liners: A Review, *Materials*, Vol. 15, No. 23, pp. 1–32, 2022, doi: 10.3390/ma15238629.
- [14] Vlădescu, S.C., Ciniero, A., Tufail, K., Gangopadhyay, A., and Reddyhoff, T.: Looking into a laser textured piston ring–liner contact, *Tribol Int*, Vol. 115, No. April, pp. 140–153, 2017, doi: 10.1016/j.triboint.2017.04.051.
- [15] Ferreira, R., Carvalho, Ó., Sobral, L., Carvalho, S., and Silva, F.: Laser texturing of piston ring for tribological performance improvement, *Friction*, Vol. 11, No. 10, pp. 1895–1905, 2023, doi: 10.1007/s40544-022-0723-5.
- [16] Etsion, I. and Sher, E.: Improving fuel efficiency with laser surface textured piston rings, *Tribol Int*, Vol. 42, No. 4, pp. 542–547, 2009, doi: 10.1016/j.triboint.2008.02.015.
- [17] Lu, P. and Wood, R.J.K.: Tribological performance of surface texturing in mechanical applications—a review, Dec. 01, 2020, IOP Publishing Ltd., doi: 10.1088/2051-672X/abb6d0.
- [18] Jiang, Y., Yan, Z., Zhang, S., Shen, Z., and Sun, H.: Research on cavitation effect of microtextured array, *Sci Rep*, Vol. 12, No. 1, Dec. 2022, doi: 10.1038/s41598-022-17258-0.
- [19] Putignano, C., Parente, G., Profito, F.J., Gaudio, C., Ancona, A., Carbone, G.: Laser microtextured surfaces for friction reduction: Does the pattern matter?, *Materials*, Vol. 13, No. 21, pp. 1–21, Nov. 2020, doi: 10.3390/ma13214915.
- [20] Vlădescu, S.C., Ciniero, A., Tufail, K., Gangopadhyay, A., and Reddyhoff, T.: Optimization of Pocket Geometry for Friction Reduction in Piston–Liner Contacts, *Tribology Transactions*, Vol. 61, No. 3, pp. 522–531, May 2018, doi: 10.1080/10402004.2017.1363930.
- [21] M, Mallikarjuna, Siddaraju, C., Kumar, H.S. and Koppad, P.: Nanohardness and wear behavior of Copper–SiC–CNTs nanocomposites, *FME Transactions*, Vol. 48, No. 3, pp. 688–692, 2020.01.01, doi: 10.5937/fme2003688M
- [22] Kuti, R.; Papp, Cs.; Tóth, M.; Tóth, Á.D.: Tribological Investigation of the Effect of Engine Oil Additives for Vintage Gasoline Engines, *FME Transactions*, Vol. 53, No. 1, pp. 31–37, 2025.01, doi: 10.5937/fme2501031K
- [23] Kuti, R.; Könczöl, F.; Csapó, L.; Papp, Cs.; Földi, L.; Tóth, Á.D.: Selection of Engine Oils with Tribological Examinations Applicable to Specially Operated Diesel Engines, *FME Transactions*, Vol. 52, No. 2, pp. 335–342, 2024, doi: 10.5937/fme2402335K
- [24] Paulovics, L.; Rohde-Brandenburger, J.; Tóth-Nagy, Cs.: Timing Chain Wear Investigation Methods – Review, *FME Transactions*, Vol. 50, No. 3, pp. 461–472, 2022, doi: 10.5937/fme2203461P
- [25] Ezhilmaran, V; Vasa, N.J.; Vijayaraghavan, L.: Investigation on generation of laser assisted dimples on piston ring surface and influence of dimple parameters on friction, *Surface and Coatings Technology*, Vol. 335, pp. 314–326, 2018, doi: 10.1016/j.surfcoat.2017.12.052
- [26] Urabe, M.; Takakura, T.; Metoki, S.; Yanagisawa, M.: Mechanism of and Fuel Efficiency Improvement by Dimple Texturing on Liner

Surface for Reduction of Friction between Piston Rings and Cylinder Bore, SAE Technical Paper, pp. 1-6, 2014, doi: 10.4271/2014-01-1661.27

- [27] Rao, X.; Sheng C.; Guo, Z.; Zhang, X.; Yin, H.; Xu, C.; Yuan, C.: Effects of textured cylinder liner piston ring on performances of diesel engine under hot engine tests, *Renewable and Sustainable Energy Reviews*, Vol. 146, 2021, 111193, doi: 10.1016/j.rser.2021.111193
- [28] Patil, S. A.; Shirsat, U.M.: Effect of laser textured dimples on tribological behavior of piston ring and cylinder liner contact at varying load, *Materials Today: Proceedings*, Vol. 44, pp. 1005-1020, 2021, doi: 10.1016/j.matpr.2020.11.172
- [29] Yin, B.; Xu, B.; Jia, H.; Zhou, H.; Fu, Y.; Hua, X.: Effects of the array modes of laser-textured micro-dimples on the tribological performance of cylinder liner–piston ring, *Proceedings of the Institution of Mechanical Engineers*, Vol. 232, No. 7, pp. 871-881, doi: 10.1177/1350650117732718
- [30] Laki, G, et al.: A Review on Friction Reduction by Laser Textured Surfaces, *Tribology Online*, Vol. 17, No. 4, pp. 318–334, 2022, doi: 10.2474/trol.17.318.
- [31] Azmi, M.A.M., Mahmood, W.M.F.W., Ghani, J.A., and Rasani, M.R.M.: A review of surface texturing in internal combustion engine piston assembly, *International Journal of Integrated Engineering*, Vol. 12, No. 5, pp. 146–163, 2020, doi: 10.30880/ijie.2020.12.05.018.
- [32] VDE VERLAG GmbH: DIN EN 60825-1, 2022, Berlin.
- [33] International Organization for Standardization: ISO 25178-2, 2021.
- [34] Dudás, A.; Laki, G.; Nagy, A.L.; Zsoldos, I.; Hanula, B.; Bartel, D.: Wear behaviour of ceramic particle reinforced atmospheric plasma spray coatings on the cylinder running surface of internal combustion engines, *Wear*, Vol. 502–503, 2022, 204373, doi: 10.1016/j.wear.2022.204373
- [35] Sharma, S., Ramakrishna, S.A., and Ramkumar, J.: Numerical simulation of melt hydrodynamics in laser micro processing of metals, *Procedia CIRP*, Vol. 95, No. March, pp. 944–949, 2020, doi: 10.1016/j.procir.2020.01.186.
- [36] Seïdgazov, R.D. and Senatorov, Yu.M.: Thermocapillary mechanism of deep melting of materials by laser radiation, *Soviet Journal of Quantum Electronics*, Vol. 18, No. 3, p. 396, 1988, doi: 10.1070/QE1988v018n03ABEH011530.
- [37] Bachchhav, B. and Bagchi, H.: Effect of surface roughness on friction and lubrication regimes, *Mater Today Proc*, Vol. 38, pp. 169–173, 2020, doi: 10.1016/j.matpr.2020.06.252.

## APPENDIX



Figure A1. Plint TE-77 High-Frequency friction machine in the Tribology Laboratory of the Department of Propulsion Technology at Széchenyi István University.

### ПРЕЛИМИНАРНА СТУДИЈА О ЛАСЕРСКОЈ ТЕКСТУРИ ПОВРШИНЕ КЛИПНИХ ПРСТЕНОВА МОТОРА ПУТНИЧКИХ АУТОМОБИЛА

Г. Лаки, Г. Ковач, А. Швајгхарт, А.Л. Нађ

Ласерско текстурирање површине нуди могуће решење за смањење трења између клизних површина у инжењерским апликацијама. Оптимизована топографија површине такође може допринети смањеном хабању и продуженом веку модификовањем стања трења у зависности од оптерећења и брзине у систему. Ова прелиминарна експериментална студија истражује применљивост приступачних система ласерског обележавања влакана за микротекстурирање клипних прстенова, како би се постигло мерљиво смањење трења у условима модела подсистема. Избор текстура се примењује на клипне прстенове од ливеног гвожђа обложене хромом. Резултирајуће топографије површине су окарактерисане конфокалном микроскопијом и подвргнуте тестирању трења. Спроведена је корелациона анализа параметара топографије површине да би се идентификовали кључни параметри ласерског процеса. Налази указују на побољшање у распону од 7-8% у погледу коефицијента трења уз одговарајућу величину текстуре.